Fresenius J Anal Chem (2000) 368 : 595–600

ORIGINAL PAPER

R. E. Ferreyra · J. M. Camiña · E. Marchevsky
J. M. Luco

Simultaneous spectrophotometric determination of La, Ho, Mn 5-Br-PADAP complexes using multivariate calibration with partial least-squares (PLS) data evaluation

Received: 28 March 2000 / Revised: 26 June 2000 / Accepted: 28 June 2000

Abstract A simple and fast analytical pocedure is proposed for the simultaneous spectrophotometric determination of lanthanum, holmium and manganese in synthetic ceramics, ($La_{(0.8-x)}$ Ho_x $Sr_{0.2}$ MnO_3), by using the partial least-squares (PLS) method. As chromogenic agent 5-Br-PADAP [2-(5-bromo-2-pyridylazo)-5-diethylaminophenol] was used, which form colored complexes with the three elements studied. To avoid metal hydrolysis, a mixture of ethanol and Triton X-100 at pH 9.5 was used for all experiments. A set of 17 calibration solutions measured throughout the 400–700 nm wavelength range was used in the calibration step. The concentration range for Mn(II) was $1–12 \times 10^{-6}$ mol L^{-1}, while the range for the rare earth elements La(III) and Ho(III) was $2–8 \times 10^{-6}$ mol L^{-1}. In order to demonstrate the applicability of the proposed method, a set of artificial samples containing the three analytes in variable proportions was prepared and analyzed. The analytical results obtained were quite acceptable with relative errors not greater than 7% in most cases.

1 Introduction

The rare-earth elements (REE) are important components of metallurgical materials and they are also used for specific technologies. The presence of trace quantities of REE in high-purity metals, semiconductors and glasses have an important influence on the electrical, magnetic, mechanical, nuclear and optical properties of these materials [1].

Great interest in new ceramic materials, which exhibit excellent electrical and magnetic properties, has been renewed after the appearance of perovskite like $La_{(1-x)}$ XR MnO_3. (where X = Ca, Ba, Sr, Pb, etc., and R = Pr, Nd, Gd, Ho, etc). These substituted compounds combine an optimum resistivity and giant magnetoresistance behavior, particularly for room temperature applications [2–4].

In previous works [5–8] we have studied some physicochemical properties of 2-(5-bromo-2-pyridilazo)-5-diethylaminophenol (5-Br-PADAP) and 2-(5-chloro-2-pyridilazo)-5-dimethylaminophenol (5-Cl-DMPAP) reagents and we have also described the experimental conditions for the spectrophotometric determination of REE and transition elements in aqueous solution. Both chromogenic agents react with several metal ions to form intensely colored complexes which have been used as a basis for diverse spectrophotometric determinations. However, due to the similarity in the chemical properties of REE, the use of techniques of relatively low cost (such as spectrophotometry) for the multicomponent analysis of REE and transition elements often cannot be carried out successfully without previous chemical separations [9]. This lack of selectivity is a common property for all pyridylazo compounds which have an hydroxyl group in the o-position to the azogroup in the benzene ring. Difficulties arise when the elements (often complexed) give partly or fully overlapped spectra. There is, therefore, a need for new and straightforward methods for the specific and economical determination of these analytes. Thus, a spectrophotometric method with an appropriate mathematical support may be a good starting point for such a development.

It is well known that the resolution of the components, whose analytical signals are partly or fully overlapped, can be improved using multivariate calibration methods. The application of the partial least squares (PLS) method, which is a full-spectrum method, is particularly well suited for systems exhibiting considerable overlapped absorption bands, since it circumvents some of the limitations of other

R. E. Ferreyra · J. M. Camiña
Departamento de Química,
Facultad de Ciencias Exactas y Naturales,
Universidad Nacional de La Pampa, Argentina

E. Marchevsky
Área de Química Analítica, Facultad de Química,
Bioquímica y Farmacia, Universidad Nacional de San Luis,
Chacabuco y Pedernera 5700 San Luis, Argentina

J. M. Luco (✉)
Laboratorio de Alimentos, Facultad de Química,
Bioquímica y Farmacia, Universidad Nacional de San Luis,
Chacabuco y Pedernera 5700 San Luis, Argentina

methods that are frequently used, such as multiple linear regression [10–13].

In this work, a spectrophotometric method in conjunction with a multicalibration approach partial least squares (PLS) method was applied to the analysis of ternary synthetic mixtures of two rare earth elements (La and Ho) and a transition metal (Mn), which are the basic elements of this class of ceramics ($La_{(0.8-x)}\,Ho_x\,Sr_{0.2}\,MnO_3$).

The 5-Br-PADAP reagent was used for the spectrophotometric determination of these elements in concentrations ranging from $1–12 \times 10^{-6}$ mol L^{-1} for Mn and $2–8 \times 10^{-6}$ mol L^{-1} for La and Ho. Besides, the influence of chemical variables affecting the reaction (such as pH, time, ionic strength, presence of detergents and suitable amounts of Sr) was also studied.

2 Theoretical background

2.1 Spectrophotometric data

The method assumes that absorbance of the mixture at any wavelength is the sum of absorbances of each formed chelate. At the j^{th} wavelength, the absorbance addition A_j will be:

$$A_j = A_1bC_1 + \ldots\ldots\ldots + A_nbC_n$$

where the subscript indicates the number of samples from *1* to *n*.

For pH 9.5, the absorption spectra for the La(III), Ho(III), and Mn(II) 5-Br-PADAP complexes are shown in Fig. 1. As can be seen, the Mn(II) and Ho(III) complexes exhibit very similar spectral characteristics over the whole 400–700 nm wavelength range. On the other hand, the La(III) complex overlaps with the other two mentioned complexes at wavelengths between 500 and 640 nm. Thus, the simultaneous determination of these ions by conventional spectrophotometric methods is hindered by strong spectral overlap in the wavelength range of 400–700 nm. However, such a determination could theoretically be facilitated by the use of multivariate calibration methods.

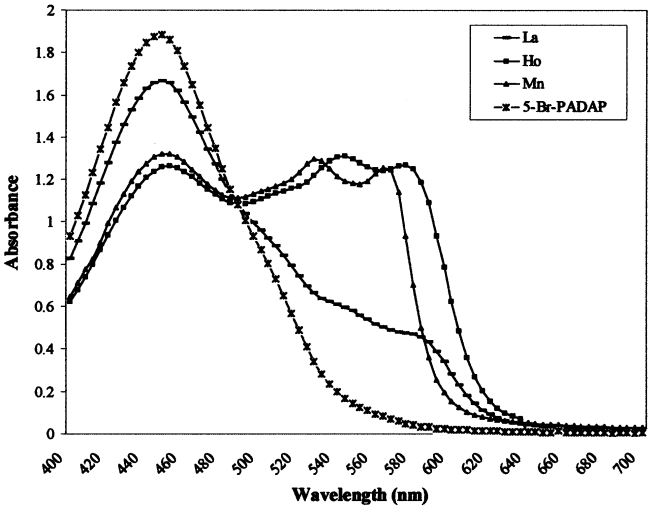

Fig. 1 Spectral curves of 5-Br-PADAP and 5-Br-PADAP complexes of lanthanum, holmium and manganese. pH = 9.5. $C_{5\text{-Br-PADAP}} = 1 \times 10^{-4}$ mol L^{-1}, $C_{La} = 1 \times 10^{-5}$ mol L^{-1}, $C_{Ho} = 1 \times 10^{-5}$ mol L^{-1}, $C_{Mn} = 1 \times 10^{-5}$ mol L^{-1}

2.2 PLS method

This principal component-like method [14–17] is based on the projection of the original multivariate data matrices down onto smaller matrices (**T,U**) with orthogonal columns, which relates the information in the response matrix **Y** to the systematic variance in the descriptor matrix **X**, as shown below:

$$\mathbf{X} = \bar{\mathbf{X}} + \mathbf{TP'} + \mathbf{E}$$

$$\mathbf{Y} = \bar{\mathbf{Y}} + \mathbf{UC'} + \mathbf{F}$$

$$\mathbf{U} = \mathbf{T} + \mathbf{H} \text{ (the inner relation)}$$

wehre $\bar{\mathbf{X}}$ and $\bar{\mathbf{Y}}$ are the corresponding mean value matrices, **T** and **U** are the matrices of scores that summarize the *x* and *y* variables, respectively, **P** is the matrix of loadings showing the influence of the *x* in each component, **C** is the matrix of weights expressing the correlation between **Y** and **T**(**X**) and **E, F,** and **H** are the corresponding residual matrices. The PLS calculations also give an auxiliary matrix **W** (PLS weights), which expresses the correlation between **U** and **X** and is used to calculate **T**. In the present work, the response matrix **Y** consisted of three dependent variables (the concentration of each analyte) while the matrix **X** consisted of the absorbance data. Determinations of the significant number of model dimensions was made by crossvalidation.

PLS analysis was carried out using both, the UNSCRAMBLER® 6.11 software package obtained from CAMO AS, Norway, and the SIMCA 7.0 software package obtained from Umetri AB, Box 7960, 907 19 Umea, Sweden.

3 Experimental

3.1 Apparatus. The measurements were performed with a Hewlett Packard (HP-8452A model) spectrophotometer equipped with a diode array wavelength detector and a Hewlett Packard printer (ThikJet model).

All measurements were made with 1.00-cm optical-path quartz cells, and the pH adjustment was performed with an Orion EA940 pH meter digital equipped with a combined glass electrode and an internal reference Ag-AgCl electrode. The potentiometer was calibrated with three buffer solutions of pH values 4.05, 7.01 and 9.8, respectively.

3.2 Reagents. A 2×10^{-3} mol L^{-1} 5-Br-PADAP (Merck) solution was prepared by dissolving an accurately weighed amount of reagent in ethanol (Merck). Lower concentrations were prepared by successive dilutions.

Standard solutions of La, Ho and Mn were prepared at 2.5×10^{-4} mol L^{-1} by dissolving suitable amounts of their nitrates (Merk) in redistilled water. All solutions (samples and standards) were prepared by adding $SrCl_2$ (Mallinckrod), at a final concentration of

1.5×10^{-5} mol L^{-1} to show that Sr(II) does not interfere in the analysis.

A buffer solution (pH 9.5) was prepared with borax and NaOH reagents (Merck). The ionic strength generated by the dissolution of ceramics in acid media, was simulated by adding $NaClO_4 \cdot H_2O$ (Merck) at 0.1 mol L^{-1}. To avoid a metal hydrolysis, a mixture of ethanol and Triton X-100 was used [18]. All solutions (samples and standards) were prepared by adding this mixture at a final concentration of 5% (v/v) ethanol and 0.5% (v/v) Triton X-100. All chemicals and solvents used were of analytical quality and redistilled water was employed in all cases.

3.3 General procedure. To 25 mL volumetric flasks were added 5 mL of sodium tetraborate/NaOH buffer at pH 9.5, appropriate volumes of the La(III), Ho(III) and Mn(II) standard solutions in such way that their final concentrations lay within the desired range, and the required amounts of 5-Br-PADAP, ethanol, $NaClO_4$ and Triton X-100. Spectra for the mixtures studied were recorded between 400 and 700 nm taking absorbance data at 2 nm intervals, and the readings were made at constant time to allow stabilization of the formed complex. The calibration and prediction procedures were carried out by using 17 calibration standards and 6 synthetic samples (ternary mixtures) prepared with different concentrations of each metal, giving final concentrations of 1.6×10^{-5} mol L^{-1} in each case (standards and samples).

4 Results and discussion

4.1 Optimization of the measurement conditions

Prior to attempting mixture resolution, we studied the stability of the different formed complex species between 5-Br-PADAP and La(III), Ho(III), Mn(II) as a function of pH, time, ionic strength, presence of tensoactive substances and suitable amounts of Sr.

The variation in absorbance of the La(III) and Ho(III)-5-Br-PADAP complexes with pH fits an inverted bell-shaped curve with a flat zone in the pH range from 9.0 and 10.9. Below pH 7 no significant complexes were formed between La(III) and Ho(III) and the reagent. On the other hand, because the Mn(II)-5-Br-PADAP complex showed good absorbances values in this pH range, a pH value of 9.5 was selected. Regarding the temporal stability, an optimum reaction time of 15 min was selected for subsequent experiments.

To avoid the hydrolysis of the formed complexes at pH 9.5, a mixture of 5% ethanol and 0.5% Triton X-100 was used. This mixture not only avoided the hydrolysis, but also improved the absorption properties of the complexes [19].

For 5-Br PADAP, the optimum ligand/metal ratio was found to be 1:2. In order to ensure a small excess of chelating agent, we adopt a ratio of 3:1 in all experiments. The influence of the ionic strength was studied to simulate an acid attack in the sample. We found no variation in the absorbance values for synthetic samples after adding increasing amounts of $NaClO_4$. For this reason, all calibration solutions and samples were used with 0.1 mol L^{-1} of $NaClO_4$. We also evaluated the influence of Sr(II) in standards and samples. However, this element does not form complexes with 5-Br-PADAP. This was demonstrated by adding 1.5×10^{-6} mol L^{-1} of $SrCl_2$ to all standards and samples corresponding to the same final concentration as the metals under study.

4.2 Effect of concomitant ions

Under the experimental conditions, the influence of some anions, cations and a number of complexing species that could be used as selective masking agents were examinated. Those influences were studied individually. The Sr(II) concentrations were kept fixed while the possible interferent

Table 1 Tolerance for some common anions

ION	Tolerated molar ratio Ion/Ho,La, Mn,Sr	Tolerated weight ratio Ion/Ho(III), La(III), Sr(II), Mn(II)			
		Ho(III)	La(III)	Sr(II)	Mn(II)
Chloride	10,000	2,150	2,520	4,034	6,454
Nitrate	10,000	3,757	4,460	7,045	11,272
Tetraborate	5,000	4,533	5,381	8,500	13,600
Acetate	5,000	5,515	6,546	10,341	16,545
Perchlorate	10,000	6,030	7,158	11,307	18,090
Bromide	500	242	288	454	727
Carbonate	100	36	43	68	109
Sulfate	1,000	581	690	1,090	1,745
Iodide	500	385	457	721	1,154
Tartrate	500	455	539	854	1,363
Nitrite	1,000	279	331	523	836
Citrate	100	116	138	218	149
Fluoride	1	Interferes	Interferes	Interferes	Interferes
Oxalate	1	Interferes	Interferes	Interferes	Interferes
Phosphate	1	Interferes	Interferes	Interferes	Interferes
EDTA	1	Interferes	Interferes	Interferes	Interferes
CDTA	1	Interferes	Interferes	Interferes	Interferes

Table 2 Tolerance for some common cations

ION	Tolerated molar ratio Ion/Ho,La, Mn,Sr	Tolerated weight ratio Ion/Ho(III), La(III), Mn(II)		
		Ho(III)	La(III)	Mn(II)
K (I)	10,000	2,363	2,805	7,090
Ca (II)	3,000	727	863	2,182
Li (I)	3,000	127	151	382
Sr (II)	3,000	1,592	1,890	4,778
Mg(II)	1,000	147	174	442
Al(III)	1,000	163	194	491
Ba(II)	1,000	832	987	2,496
Au(III)	50	59	70	179
Si(IV)	1,000	169	201	509
Be(II)	200	11	13	32
W(VI)	200	222	264	668
Te(IV)	200	154	183	464
Zr(IV)	200	110	131	331
Ru(III)	50	30	36	92
Rh(III)	50	312	370	935
Cr(III)	50	16	18	47
As(III)	50	22	27	68
Zn(II)	1	Interferes	Interferes	Interferes
Cu(II)	1	Interferes	Interferes	Interferes
Ni(II)	1	Interferes	Interferes	Interferes
Bi(III)	1	Interferes	Interferes	Interferes
Fe(III)	1	Interferes	Interferes	Interferes
Pb(II)	1	Interferes	Interferes	Interferes
Pd(II)	1	Interferes	Interferes	Interferes
Sb(III)	1	Interferes	Interferes	Interferes
Co(II)	1	Interferes	Interferes	Interferes
U(VI)	1	Interferes	Interferes	Interferes
Th(IV)	1	Interferes	Interferes	Interferes
V(V)	1	Interferes	Interferes	Interferes
Lanthanide	1	Interferes	Interferes	Interferes

was increased until the magnitude of error was ca. 5%, arbitrarily established as the maximum acceptable. Table 1 shows the admissible proportions of several anions and masking agents and Table 2 shows the admissible proportions of several cations. Inspection of the data in these tables reveal that EDTA, CDTA and phosphate interfere in a molar ratio lower than 1:1 with respect to Ho(III), La(III) or Mn (II). On the other hand, cations as Bi(III), Cd(II), Cu(II), Fe(III), Ni(II), Pb(II), Sb(III) and Zn(II) ions cannot be present in a ratio 1:1 because they interfere seriously. Finally, most REE react with 5-Br-PADAP resulting in serious interferences with the determination of La(III), Ho(III) and Mn(II). Therefore, a separation technique has to be used or, as in this work, a multivariate calibration method that permits to treat complex mixtures of analytes with similar spectral characteristics.

4.3 PLS analysis of ternary mixtures: calibration set

All variables (absorbance and concentration matrices) used in the PLS calculations were initially autoscaled to zero mean and unit variance. The statistical significance of the screened models was judged by the correlation coefficient (r), the root mean square error (RMSE) and the F-statistic. The predictive ability was evaluated by the crossvalidation coefficient (Q) which is based on the prediction error sum of squares (*PRESS*):

$$PRESS = \sum_{i=1}^{n} \left(\bar{c}_i - c_i\right)^2$$

where $\bar{c}_i$ is the predicted concentration in sample *i*; c_i is the actual concentration and n is the number of samples. The number of significant PLS components was determined using the crossvalidation procedure, leaving out one sample at a time and calculating the *PRESS* each time a new factor is added. On the other hand, the VIP (variable importance for the projection) parameter [20] was used to unravel which wavelength range was the most relevant to explain the Y concentration matrix. The SIMCA program computes the influence on the Y matrix of every term (x_k) in the model, called VIP. This is the sum over all model dimensions of the VIN (variable influence) contributions. For a given PLS dimension, a, $(VIN)_{ak}^2$ is equal to the

Table 3 Experimental and calculated concentration values for La, Ho and Mn (10^{-6} M) in the calibration matrix

	La (obs.)	La (cal.)	Ho (obs.)	Ho (cal.)	Mn (obs.)	Mn (cal.)
1	2	2.3	2	1.7	12	12
2	3	3	3	3	10	10
3	4	4.1	4	4	8	8
4	5	5	5	4.9	6	6.1
5	6	6.1	6	5.9	4	4
6	7	7.3	7	6.8	2	2
7	8	7.8	6	6	2	2.1
8	7	6.9	5	5.2	4	3.9
9	4	4	6	6	6	6
10	6	5.8	4	4.3	6	5.9
11	5	4.8	6	6.3	5	4.9
12	6	6.1	5	5.1	5	4.8
13	6	6.3	7	6.8	3	2.9
14	8	8.1	7	6.9	1	1
15	7	6.8	8	8.1	1	1.1
16	2	2	3	3.1	11	10.9
17	3	2.8	2	2.1	11	11.1

squared PLS weight $(w_{ak})^2$ of that term, multiplied by the percent explained, *SS*, for that PLS dimension. The accumulated overall PLS dimension, $VIP_{ak} = [VIN]_{ak}^2$, is then divided by the total percent explained, *SS*, for the PLS model and multiplied by the number of terms in the model.

The calibration matrix was constructed with 17 calibration standards. The selected concentration ranges were from 2×10^{-6} mol L^{-1} to 8×10^{-6} mol L^{-1} for La(III) and Ho(III); and 1×10^{-6} mol L^{-1} to 12×10^{-6} mol L^{-1} for Mn(II). Preliminary analysis of the obtained PLS models showed that the useful wavelength range was from 520 to 616 nm. The composition of the calibration matrix of the ternary mixture is given in Table 3.

The PLS analysis for the calibration matrix resulted in a significant two-component model with the following statistics: r = 0.997, Q = 0.996, RMSE(La) = 0.0018, RMSE(Ho) = 0.0018, RMSE(Mn) = 0.0009. The model accounted for 99.5% (99.3%, 99.2% and 99.9%, respectively) of variance in the Y concentration matrix. Most of the spectral variation in X was accounted for the first PLS component (R^2X = 0.911) which besides, gave a sufficiently good fit to the Y matrix (R^2Y = 0.926). However, internal crossvalidation indicated that the second PLS component reflects significant amounts of information (R^2X = 0.088, R^2Y = 0.068 and Q^2 = 0.917). It is important to note that the third PLS component was not significant to explain the X and Y matrices (R^2X = 0.0001, R^2Y = 0.001 and Q^2 = –0.438). Figure 2 shows the obtained RMSE values for the ternary mixture in the calibration process and Fig. 3 shows the loadings of the PLS model. The loading plot shows the main relationships between the X and Y matrices and as can be seen, a causal interpretation of each individual PLS component is rather difficult. The loadings of the first PLS component show that

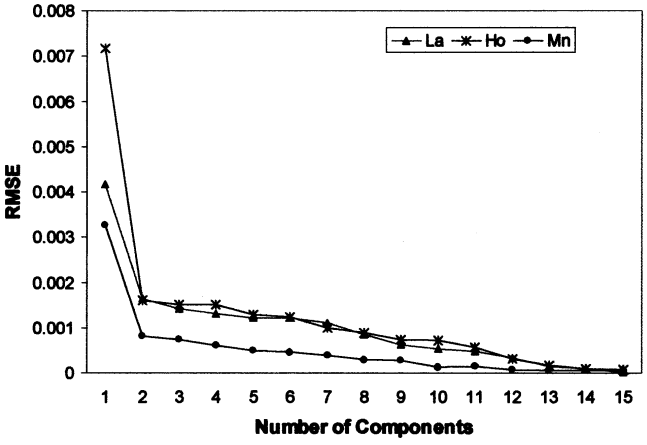

Fig. 2 RMSE values as a function of the number of PLS components used in the calibration process

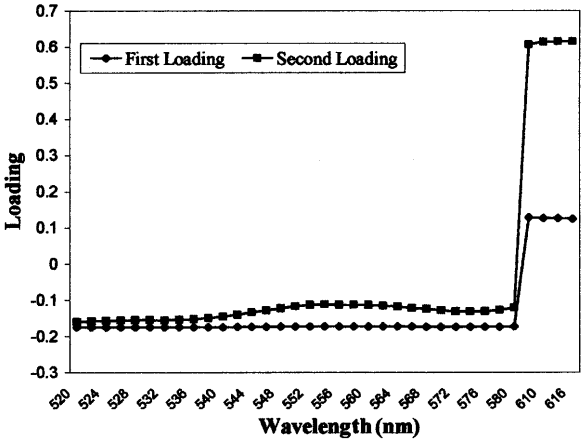

Fig. 3 Loading plot as a function of the wavelength (matrix X)

the 520–580 nm wavelength range correlated the same way while the spectral range of 580–616 nm only represents minor contributions to this factor. The loadings of the second PLS component show that the 580–616 nm wavelength range has the largest contribution, which could be related to the greater spectral difference observed between the Ho(III) and Mn(II) complexes (see Fig. 1). Finally, the residual values showed a reasonable central tendency and the agreement between the measured and calculated values was very good as shown in Table 3.

4.4 Model validation: sample set

It is well known that the real predictive ability of any calibration PLS model cannot be judged solely by using internal validation (i.e., crossvalidation); it has to be validated on the basis of predictions for compounds not included in the calibration set [21]. Thus, in order to demonstrate the applicability of the proposed method, a set of artificial samples containing the three analytes in variable

Table 4 Experimental and calculated concentration values and relative error (%) for La, Ho and Mn (10^{-6} M) in the synthetic samples

	La (obs.)	La (pred.)	% rel. error	Ho (obs.)	Ho (pred.)	% rel. error	Mn (obs.)	Mn (pred.)	% rel. error
1	6	6.3	5	8	7.6	5	2	2.1	5
2	5	5.4	8	7	6.6	5.7	4	4	0
3	7	7.2	2.8	6	5.9	1.6	3	2.8	6.6
4	4	4	0	7	7	0	5	5	0
5	3	2.7	10	4	4.2	5	9	9.1	1.1
6	8	7.8	2.5	6	6.1	1.6	2	2.1	5

proportions was prepared and analyzed. Table 4 shows the results obtained by applying the developed PLS model. As can be seen, the relative errors were quite acceptable as they were not greater than 7% in most cases.These results justify that the calibration PLS model evaluated is not overfitted and has a good predictive ability, which permits its use for analytical purposes.

5 Conclusions

Based on the results, the proposed spectrophotometric method permits the simultaneous determination of lanthanum, holmium and manganese in perovskite like $La_{(0.8-x)}\,Ho_x\,Sr_{0.2}\,MnO_3$. The proposed method can be used without previous chemical separations and has the advantage of combining high sensitivity and low cost equipment. Further, this fact provides evidence for the great potential of the PLS method to treat complex mixtures of analytes which exhibit similar spectral characteristics.

The developed method provides expeditious and precise results and is suitable for the routine analysis of this class of ceramic materials.

Acknowledgements We thank Prof. Dr. Roberto Olsina for careful reading of the manuscript and for his friendly support. We are also grateful to Universidad Nacional de San Luis, Universidad Nacional de La Pampa and CONICET.

References

1. Kantipuly CJ, Westland AD (1988) Talanta 35 (1):1–13
2. Sharma N, Nigam AK, Pinto R, Venkataramani N, Prasad S, Chandra G, Pai SP (1997) J Magn Mater 166:65–70
3. Gubkin MK, Perekalina TM, Chubarenko VA, Shapiro AY (1995) Phys Solid State 37(4): 600–602
4. Broekaert JAC, Graule T, Jenett H, Tölg G, Tschöpel P (1989) Fresenius Z Anal Chem 332: 825–838
5. Martinez L, Olsina R, Marchevsky E, Delfino M (1993) Int J Chem 4(3): 87–95
6. Martinez L, Olsina R, Marchevsky E, Delfino M (1995) Int J Chem 6(3): 79–88
7. Martinez L, Perino E, Marchevsky E, Olsina R (1998) J Trace Microprobe T 16(3): 353–361
8. Zucchi C, Forneris M, Martinez L, Olsina R, Marchevsky E (1998) Fresenius J Anal Chem 360:128–130
9. Kubán V, Gladilovich D (1988) Collect Czech Chem Commun 53:1664
10. Sharaf MA, Illman DL, Kowalski BR (1986) Chemometrics, John Wiley & Sons, New York
11. Thomas EV (1994) Anal Chem 66 (15): 795A–804A
12. Luco JM, Ferretti HF (1997) J Chem Inf Comput Sci 37: 392–401
13. Luco JM (1999) J Chem Inf Comput Sci 39: 396–404
14. Beebe KR, Pell RJ, Seasholtz MB (1998) Chemometrics: a Practical Guide. John Wiley & Sons Ltd, New York
15. Kramer R (1998) Chemometric Techniques for Quantitative Analysis. Marcel Dekker, Inc, New York
16. Martents H, Naes T (1996) Multivariate Calibration. John Wiley & Sons Ltd, New York
17. Beebe K, Kowalski B (1987) Anal Chem 59 (17):1007A–1017A
18. Savvin S, Chernova K (1979) Micellar Reactions in Spectrophotometric Analysis. Plenum Publishing Corporation, pp 51–60
19. Martinez L, Perino E, Marchevsky E, Olsina R (1993) Talanta 40 (3):385
20. Wold S (1995) In: van de Waterbeemd H (ed) Chemometric Methods in Molecular Design, Vol 2 Chapter 4.4 p 195–218
21. Wold S, Eriksson L (1995) In: van de Waterbeemd H (ed) Chemometric Methods in Molecular Design, Vol 2 Chapter 5.1 p 309–318